Absorption of femtosecond laser pulses in interaction with solid targets

Q. L. Dong, J. Zhang,* and H. Teng
Laboratory of Optical Physics, Institute of Physics, Chinese Academy of Sciences, Beijing 100080, China
(Received 4 April 2001; published 24 July 2001)

We have studied the effects of the plasma density scale length on the absorption mechanism of the femtosecond (fs) laser pulses interacting with solid targets. Experiments and particle-in-cell (PIC) simulations demonstrate that the vacuum heating is the main absorption in the plasma in the interaction of fs laser pulses with solid targets when no prepulses are applied. The energy spectrum of hot electrons ejected out of or injected into the plasma show a bitemperature distribution. While the first temperature of the two groups of hot electrons can be attributed to the ''pull-and-push'' exertion of the laser field, the second temperature refers to the electrons accelerated by the static part (in front of the target) and the oscillating part (in the plasma layer) of the laser-induced electric field, respectively. PIC simulations also show that with an appropriate density scale length, the femtosecond laser energy can be absorbed locally through different mechanisms.

DOI: 10.1103/PhysRevE.64.026411 PACS number(s): 52.38.−r, 52.50.Jm, 52.65.Rr

I. INTRODUCTION

The research of the femtosecond laser-plasma interaction is of importance because of many potential applications, such as the fast ignition scheme of inertial confinement fusion [1], plasma-based particle accelerator [2], and coherent x/γ ray sources [3], etc. The laser-produced plasmas also provide a test bed for the high temperature, high-density plasmas relative to some astrophysical phenomena [4]. Those topics are strongly dependent on the laser energy absorption in plasmas [5–12]. However, with long laser pulses, the plasma evolution during the duration of the laser pulse makes the physical process in the laser-plasma interaction very complex. The recent availability of the intense ultrashort lasers with chirped pulse amplification (CPA) [13] has enabled the investigation of different physics mechanisms by significantly reducing the hydrodynamic effects of plasmas during the interaction. In this paper, we report our study on the absorption mechanism in the interaction between femtosecond laser pulses and plasmas with various density scale lengths. In Sec. II, the vacuum heating (VH) mechanism is demonstrated to be responsible for the absorption through particle-in-cell (PIC) simulations and laboratory experiments for an abrupt density profile in the interaction between femtosecond laser pulses and solid targets. We will show that the laser-induced longitudinal electric field perpendicular to the target surface plays an important role in the electron acceleration and the laser absorption. In Sec. III, the effects of the density scale length on the absorption mechanism are investigated using PIC simulation. The laser energy can be absorbed locally if an appropriate density scale length is used.

II. ABSORPTION AT THE PLASMA SURFACE

The absorption mechanism for ultrashort laser pulses irradiating on solid targets or a plasma with a very steep electron density profile was studied by several authors [5–7,9,10]. At normal incidence for intermediate intensities, the dominant absorption mechanism includes the normal skin effect ($eE_0/m\omega_0^2 \ll v_{th}/\nu \ll l_s$), the anomalous skin effect ($v_{th}/\nu \gg eE_0/m\omega_0^2 \gg l_s$) [9], and the sheath inverse bremsstrahlung absorption SIB ($eE_0/m\omega_0^2 \ll l_s \ll v_{th}/\nu$) [10], etc. Here e, m, and v_{th} are the charge, mass, and thermal velocity of electrons. E_0 and ω_0 is the electric field amplitude and the cycle frequency of the laser field, respectively. ν is the collision ratio between electrons and ions in the skin layer of the plasma with a thickness of l_s. However, the interaction process between a p-polarized laser pulse and a plasma with steep density profile differs much in that the electric field of the laser, which has component perpendicular to the target surface, can directly pull electrons out of and send them into the plasma. If the excursion length of electrons in the laser field during one cycle, i.e., $r_0 = eE_0/m\omega_0^2$, exceeds the density scale length of the plasma $L = (\partial \ln n_e/\partial x)^{-1}$, those electrons will then deposit their quivering energy into the over-dense plasma where the laser field can not penetrate into. Such an absorption process is called VH and was first predicted by Brunel [5], and then studied further by Gibbon [6] and Kato [7]. This topic is still worthy of further investigation because some physical processes are still unclear to us, for example, the electron acceleration mechanism under such conditions. Furthermore, there are few experiments devoted to the investigation of this absorption mechanism of ultrashort laser pulses directly interacting with solid targets due to the difficulties to measure the electron density scale length. But such problem is solved perfectly by the technique of frequency domain interferometry to give 0.01λ resolution or better [14].

In this section, we first give out some characteristics of VH obtained through PIC simulations, then by combining experiments and PIC simulations, we demonstrate the vacuum heating mechanism of the ultrashort laser pulse on solid target surface.

A. Vacuum heating in PIC simulations

We used a 1D3V relativistic electromagnetic PIC code LPIC++ [15] to simulate fs laser pulses interacting with a

*Author to whom correspondence should be addressed. Electronic address: jzhang@aphy.iphy.ac.cn

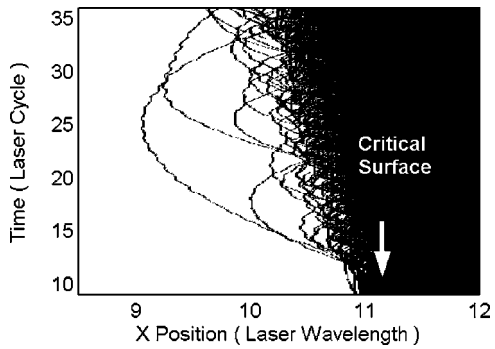

FIG. 1. Electron orbits in the space-time coordinate.

solid target. In order to understand the detailed process of laser absorption, most PIC variables are initialized based on the conditions of the experiments conducted at our laboratory for better comparison of PIC simulations with laboratory experiments. The simulation box has a length of 20.5λ along the x direction. A region of 5.5λ in the middle of the box is occupied by the plasma with an electron density rising exponentially from $0.01n_c$ at the point of 10λ to $35n_c$ with a scale length L of 0.04λ. Here, n_c is the critical density for the laser pulses with a wavelength of λ. The initial electron temperature was set to be 100 eV and ions are mobile [16]. A p-polarized fs laser pulse was launched from the left boundary at an incidence angle of 45° between the laser propagation and x direction. It has a duration of 56 periods and a relativistic intensity of 0.06, corresponding to the conditions of our experiments of laser wavelength, duration, and intensity of 0.8 μm, 150 fs and 5×10^{15} W μm^2 cm^{-2}, respectively.

For the intensity and time scale studied here, the produced plasma has little time to expand and the electrons' quiver amplitude r_0 and the density scale length L satisfy the condition of $r_0/L>1$. This suggests that the classical resonance absorption is weak, because as a collective action, plasma oscillation needs the particles ''keeping in order'' for a time long enough so that its amplitude grows in a space interval at the critical density position where the plasma frequency equals to the driver frequency [8]. However under the conditions we consider here, the electrons are pulled out of targets in the first half of the laser cycle. Some of them are sent back again in the same cycle, while others stay out of the target until several laser cycles later. Figure 1 shows the electron orbits in the space-time coordinates. The fact that these electrons have the parabolic orbits suggests that there is a force pointing to the target. In order to understand this phenomenon, we diagnose the laser-induced electric field through the simulation box, and obtain the snapshot of its component E_x perpendicular to the target surface, which is shown in Fig. 2(a). It can be seen clearly that a negative electric field locate in front of the target. The spectrum of E_x shows a zero component indicating that the negative electric field exists in the laser-plasma interaction process. It is the negative electric field that results in the electron parabolic orbits. Obviously, the negative electric field is induced by the charge separation as some electrons are pulled out and staying out of the plasma, constituting an electron cloud in front

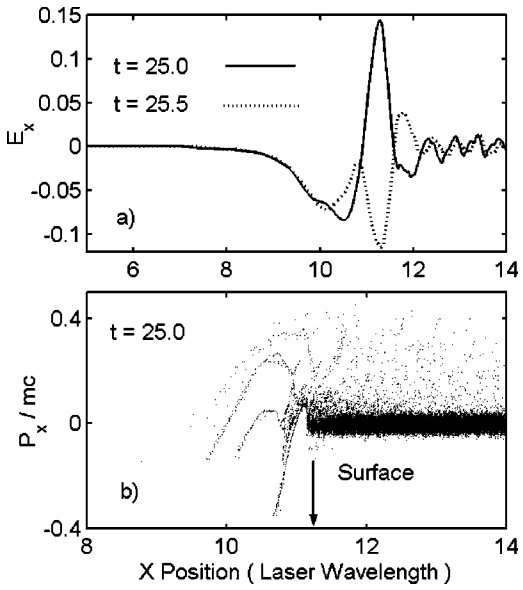

FIG. 2. Laser-induced longitudinal E_x (a) and the electron phase space (b) in the 25th laser cycle.

of the target, while ions stay at their original position due to their great mass ratio to electrons. This electron cloud plays an important role in the absorption of the laser energy as we can see later.

In the skin layer of the plasma, the longitudinal electric field E_x oscillates with the frequency equal to ω_0. Its maximum value here can reach 0.4 (normalized through $eE_x/m\omega_0$) with a spatial width of half of the laser wavelength along the x direction. The negative static electric field in front of the target and the oscillating part of E_x play the dominant role in accelerating electrons out of or into the plasma. In Fig. 3, we give out the simulated energy spectrum of hot electrons going out of the plasmas as well as an experimental one measured using a magnetic spectrometer set in front of the target in the normal direction. Both spectra show a bitemperature structure. The two equivalent temperatures are determined from the quasiexponential slope. The first temperature T_{h1} refers to electrons being heated by the laser's ''pull-and-push'' exertion. However, the second temperature T_{h2} is much higher than T_{h1} and cannot be simply attributed to such a process. In fact, this group of the outgoing hot electrons is accelerated by the oscillating part of the longitudinal electric field E_x. Such electrons can overcome the static field in front of the target and be detected by the magnetic spectrometer. On the other hand, the static part of the electric field will accelerate those electrons staying out to higher energies. This can be seen as those with positive momentum up to 0.4 inside the plasma as shown in Fig. 2(b). Such energetic electrons will be decelerated in the overdense plasmas, emitting x rays from which, after deconvolution of the detector response and the transmission effects of solid targets, the temperature of hot electrons penetrating into the overdense plasma can be deduced [17]. Experiments conducted here show that the x-ray spectra also has a similar bitemperature structure with the second one referring to

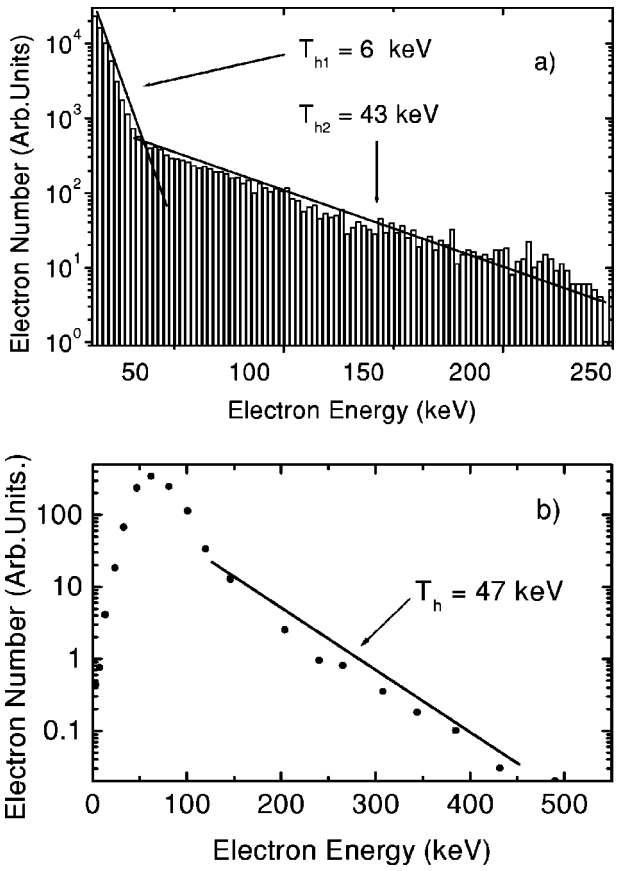

FIG. 3. The electron energy spectrum obtained from the PIC simulation (a) and the laboratory experiments (b).

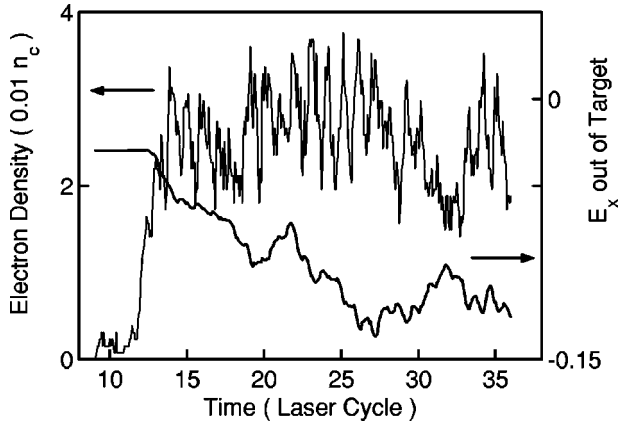

FIG. 4. The temporal evolution of the electron density and the static electric field in front of the target.

those electrons accelerated by the static field as mentioned above.

An important aspect of the physics studied here is the detailed behavior of the laser energy absorption. By monitoring the reflected laser flux at the left boundary, we get the detailed behavior of absorption during the laser-plasma interaction. In our simulations, there are two main absorption peaks during the laser-plasma interaction process. The absorption behaviors should be understood by taking into account the electron cloud in front of the targets. We get the evolution of the electron density and the laser-induced electric field in front of the targets. This is shown in Fig. 4. Once the laser begins to interact with the plasma at about tenth period, the two diagnostic variables increase gradually, and at later time corresponding to the two main absorption peaks, there are two minima (electron density) or maxima (electric field), respectively. This shows us a picture of the interaction process. Once the laser pulse reaches the plasma target, electrons are pulled out and accumulate in front of the target and a negative electrostatic field builds up as shown by Fig. 2(a). This process continues until the dc field reaches a minimum value which is about two times the longitudinal part of the laser electric component, say, $E_x = 2E_0 \sin(\pi/4)$. Then many electrons will be sent back into the plasma in groups by the charge separation potential. Since these electrons are quivering with the laser electric component, the returning electron bunch can result in great absorption of laser energy nonadiabatically. The total absorption due to the VH process can reach 46% as deduced from the ratio of the incident and reflected energy.

To ensure that our simulation with $L = 0.04\lambda$ is not a special case, we did several simulations with the same set of parameters described but with different L, which varies between 0.01λ and 0.1λ. We wish that this should reduce the density scale length difference between our simulations and the laboratory experiments. It was found that as long as L is controlled within a certain range ($L < 0.1\lambda$), the physics mechanism to produce hot electrons is independent of plasma density scale length. The main results obtained from the simulations for L between 0.01λ and 0.1λ are also the same as the case with $L = 0.04\lambda$. These simulations confirm that during the interaction between fs laser and solid targets, the vacuum heating is the main absorption mechanism.

B. The vacuum heating in experiments

The experiments were conducted at the Laboratory of Optical Physics of the Institute of Physics with a Ti:sapphire chirped pulse amplification (CPA) laser system operating at around 800 nm at a repetition rate of 10 Hz. The laser delivered 5 mJ energy in 150 fs with a peak-to-pedestal contrast ratio of 10^5 at 1 ps. The *p*-polarized laser pulse (with a polarization ratio of 95%) was focused at an incidence angle of 45° on an Al target. The target was moved in the direction parallel to the target surface to ensure that the laser pulse interacts directly with a fresh surface at each shot. By moving the target perpendicularly to the target surface, we get the focused intensities varying in the range between 5×10^{12} and 5×10^{15} W μm^2/cm^2 at the best focus. The absorption of the laser beam was determined by measuring the scattered and specularly reflected lights with a group of calorimeters. The electron density scale length is monitored by the interferometry in frequency domain.

Figure 5 gives the determined absorption (hollow-circle line) in experiments. As a comparison, we also plotted the measured absorption by the inverse bremsstrahlung (IB) process in the plasma (solid line) given by Price [18]. The great discrepancy between the two groups of data is not surprising. In order to investigate the process during the interaction, we

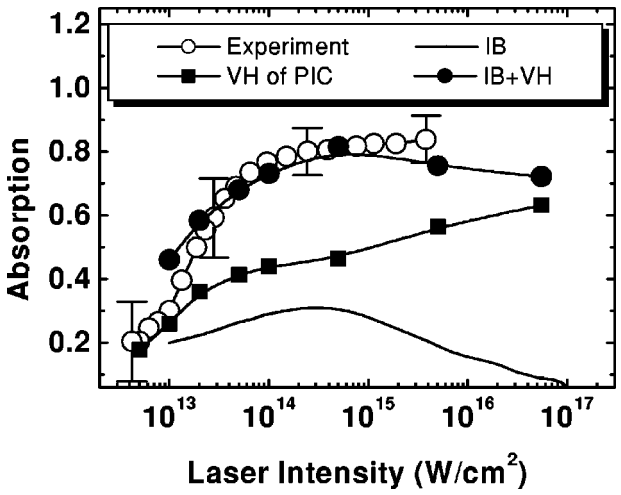

FIG. 5. Absorption ratio versus laser intensities. Our experimental value: hollow-circle line; The IB absorption [18], solid line; the VH absorption, solid-square line; the sum of VH and IB, solid-circle line. In PIC simulations, the L are applied as the following: $L=0.01\sim0.02\lambda$ when $I<10^{14}$ W/cm^2; $L=0.04\pm0.01\lambda$ for I between 10^{14} and 5×10^{15} W/cm^2; $L=0.07\pm0.01\lambda$ when $I>5\times10^{15}$ W/cm^2.

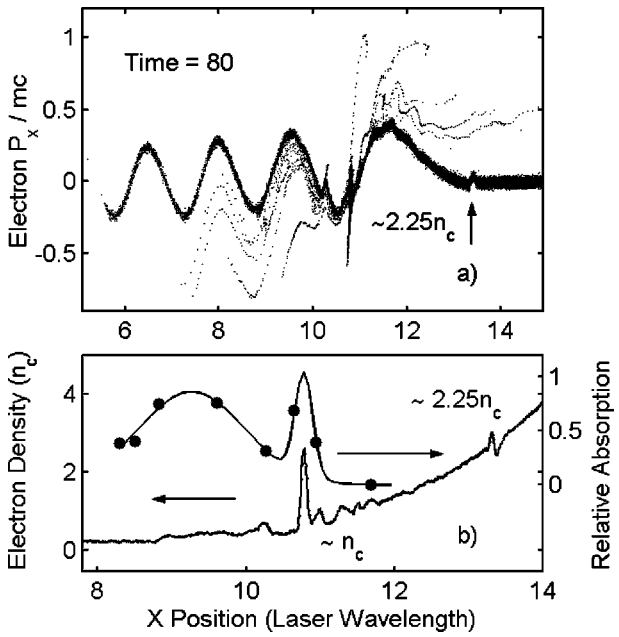

FIG. 6. The electron distribution in its phase space (a). (b) The disturbed electron density profile (solid line) and the relative absorption (solid-circle line). The parameters for the simulation are $L=2\lambda$ and $a_0=0.2$.

did some PIC simulations using the electron scale length measured by the technique of the frequency domain interferometry and the temperature deduced by supposing isothermal expansion of plasma in the experiments [19]. The values of L applied are: $L=0.01\sim0.02\lambda$ when $I<10^{14}$ W/cm^2; $L=0.04\pm0.01\lambda$ for I between 10^{14} and 5×10^{15} W/cm^2; $L=0.07\pm0.01\lambda$ when $I>5\times10^{15}$ W/cm^2. The PIC simulations show that the absorption ratio from PIC simulations at a fixed intensity is more sensitive to the density scale length L at low intensities than at high intensities. The collision between electrons and electrons/ions is not included in the PIC code. The simulation results show that, under those conditions, the vacuum heating dominates the absorption of laser pulses. After we added the experimental data of IB absorption to the values from PIC simulations and compared the sum (solid-circle line) with our experimental results, we found a good agreement. This implies that the vacuum heating does exist in the experiments at the intermediate intensities. We noticed the discrepancy at the low and high intensity end. The reasons are different and can be explained as follows. At lower intensities, the laser intensity is just over the ionization threshold. The ionization process and the intraatomic absorption play important roles in the interaction. The behavior of such plasma can not be simulated by the PIC method. At higher intensities, an overdense plasma is formed. However, because the plasma surface is disturbed by the electric component dragging electrons out of and pushing them back into the plasma, it cannot be regarded as a plasma mirror as in the experiments conducted by Price [18]. Given the IB absorption is increased due to the plasma surface disturbance, we believe that the sum of the absorption due to VH and IB will give a better agreement with our experiments at the higher intensity.

III. VOLUME HEATING OF PLASMAS

For plasmas with a larger density scale length, the absorbing region shifts from overdense plasma towards critical density with the corresponding change in the absorption mechanism, for example, change to resonance absorption (RA) when $L<1\lambda$. However, recent PIC simulations [20] and laboratory experiments by Zhang *et al.* [21] demonstrated more than one absorption peak for different scale lengths. This indicates that during the interaction between fs laser pulses and plasmas with a larger scale length $L>1\lambda$, other absorption mechanisms will play roles apart from the IB and RA. In this section, we investigate the absorption of ultrashort laser pulses by plasmas with various scale lengths. We focus on the parametric instabilities taking place in the underdense plasma.

Figure 6(a) gives the electron distribution in the phase space with the initial condition: $a_0=0.2$, $L=2\lambda$. The regular Langmiur wave breaks in the region at the critical density, causing density profile disturbance as shown by solid line in Fig. 6(b). Corresponding to the wave break, the laser pulse deposits its energy irreversibly to hot electrons in this region, limited by half of the Langmiur wavelength [solid-circle line in Fig. 6(b)]. The absorption process in this region can be considered as RA. We also find another wide absorption peak crossing the region between $0.25n_c$ and $0.5n_c$. This absorption peak should be attributed to the two-plasmon decay instability (TPD) in that the $\frac{1}{2}\omega_0$ and $\frac{3}{2}\omega_0$ components appear in the electromagnetic fields with the conversion efficiency about 1% as shown in its time integrated spectra. Indeed, with parameters mentioned above, the predicted TPD threshold in inhomogeneous plasmas is satisfied, i.e., $k_0Lv_0^2/v_{th}^2\sim4>3$. Here, $v_0=eE_0/m\omega_0$ is the electron quiver velocity

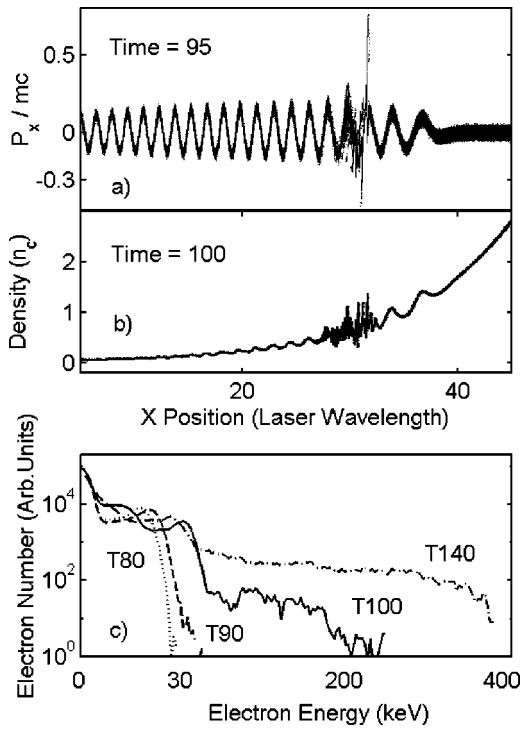

FIG. 7. The electron phase space (a), the disturbed electron density profile (b), and the temporal evolution of the electron energy distribution (c). The parameters for the simulation are $L=25\lambda$ and $a_0=0.2$.

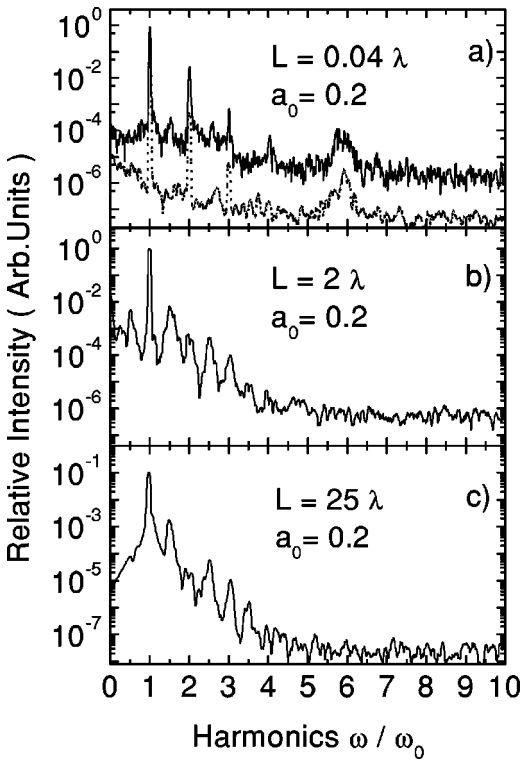

FIG. 8. The time-integrated spectra for different parameters as shown in the graphs.

in the laser field; k_0 is the laser wave number. Also, there is a disturbance at the position of $2.25n_c$ in the snapshot of the phase space [Fig. 6(a)] and on the density profile [Fig. 6(b)]. Such disturbance is caused by the $\frac{3}{2}\omega_0$ part of the electromagnetic field, which is generally considered to be the secondary signature of TPD.

It is a well known problem that the primary unstable Langmiur wave from TPD is required to propagate a distance to match with photons of frequency ω_0 to produce the $\frac{3}{2}\omega_0$ light. The disturbance of density profile at $\frac{9}{4}n_c$ also indicates the existence of the Langmiur wave propagating towards the higher density with increasing wavelength. This case is much clearer when L increases as shown in Fig. 7(a). Such Langmiur waves will be reflected at the corresponding critical surface, causing irregular density profile in a wide range from $0.5n_c$ to $0.8n_c$ which can be seen from Fig. 7(b).

The TPD parametric instability provides anomalous absorption mechanism by which laser energy is converted to that of hot electrons. Figure 7(c) gives out the temporal evolution of the electron energy spectrum, showing the sudden acceleration of electrons through wave break, producing a non-Maxwellian distribution of electrons. Such an acceleration process is quite different from that in the VH process where the hot electron energy increases gradually with time. The energetic component of the electron distribution may transport into the overdense plasma during the laser pulse. They can be used to ignite the precompressed fuel in the fast ignition scheme of the inertial confinement fusion [1]. The non-Maxwellian distribution of electrons also has a pronounced effect on the physical process in the overdense region of plasmas. For example, the ratio of some special satellite lines in the x-ray spectroscopy from the overdense plasma can be greatly enhanced [22,23]. However, the transportation of such energetic electrons may be inhibited by the self-generated magnetic field or by the local electrostatic field produced by the charge separation due to the finite conductivity of plasmas [24]. High absorption can still be achieved by the heat flow parallel to the target surface [25]. It needs at least two-dimensional PIC simulations to investigate the detail of the laser absorption at higher intensities at which the inclusion of the target deformation in consideration is necessary.

The time-integrated spectra of the reflected laser pulse are shown in Fig. 8 for three different density scale length. With a steep electron density profile, the integral harmonics of the reflected laser pulse dominate the whole spectrum as shown in Fig. 8(a). Such spectra is caused by electrons, which are pulled out of and then sent back into plasmas inducing disturbance at the plasma surface [15,26]. In the simulation with a smoother profile, the obtained spectrum is dominated by the harmonics of $\frac{1}{2}\omega_0$ [Figs. 8(b) and 8(c)], which is the consequence of TPD as demonstrated above. However, with much larger scale length $L=25\lambda$, the plasma wave and the laser pulse propagate a long distance together so that the $\frac{1}{2}\omega_0$ component is significantly reduced compared to that with $L=2\lambda$. There is also a line emission of the plasma as shown in Fig. 8(a). Such line emission is one feature of the Langmuir wave in the plasma stimulated here by the injected electrons originating from the plasma surface as shown in Fig. 1 and Fig. 2(b). A time-integrated spectra from another simulation with the same parameters but fixed ions is given as a dotted

line in Fig. 8(a) for a comparison. With ions mobile, the broadening of the harmonic lines is obvious, indicating that when studying the spectra from the plasma, it is necessary to include the ion motion especially when the laser pulse is long or very intense.

IV. CONCLUSION

In summary, we have reported our investigation of the absorption of fs laser pulses interacting with solid targets. Our experiments and PIC simulations indicate that without prepulses, the vacuum heating and the IB mechanism play the dominant role in the laser's absorption. Experiments show that the two groups of electrons ejected out of and/or injected into the plasma both have a bitemperature distribution. According to the PIC simulation, the first temperature of the ejected and injected electrons refers to electrons heated by the laser pulse's ''pull-and-push'' exertion. However, the second temperatures of such electrons are induced by different parts of the longitudinal electric field. The second temperature of hot electrons penetrating into the overdense plasma refers to those staying out of the target and being accelerated by the static electric field. On the other hand, the second temperature of out-going hot electrons refers to those accelerated by the oscillating part of the longitudinal electric field in the skin layer. We also studied the interaction between fs laser pulses and preperformed plasmas with various density scale lengths L. The PIC simulations show that fs laser pulses, interacting with plasmas with an intermediate L, can be absorbed locally along the density profile. The main absorption mechanism in this case is considered to be parametric instabilities apart from RA and IB. The time-integrated spectra of the reflected pulse are also given, confirming these absorption mechanisms discussed above.

ACKNOWLEDGMENTS

This work was jointly supported by the National Natural Science Foundation (NNSF) of China under Grants Nos. 19825110 and 10075075 and the National High-Tech ICF program and the National Key Basic Research Special Foundation (NKBRSF) under Grant No. G1999075200.

[1] M. Tabak *et al.*, Phys. Plasmas **1**, 1626 (1994).
[2] A. Modena *et al.*, Nature (London) **377**, 606 (1995), and references therein; C. L. Moore *et al.*, Phys. Rev. Lett. **79**, 3909 (1997); A. J. Mackinnon *et al.*, *ibid.* **86**, 1769 (2001).
[3] M. M. Murnane *et al.*, Science **251**, 531 (1991); J. D. Kmetec *et al.*, Phys. Rev. Lett. **68**, 1527 (1992); U. Teubner *et al.*, Phys. Rev. E **54**, 4167 (1996); M. H. Key *et al.*, Phys. Plasmas **5**, 1966 (1998); P. A. Norreys *et al.*, *ibid.* **6**, 2150 (1999).
[4] B. A. Remington *et al.*, Science **284**, 1488 (1999); J. S. Wark *et al.*, Phys. Plasmas **4**, 2004 (1997).
[5] F. Brunel, Phys. Rev. Lett. **59**, 52 (1987); Phys. Fluids **31**, 2714 (1988).
[6] P. Gibbon and A. R. Bell, Phys. Rev. Lett. **68**, 1535 (1992); P. Gibbon, *ibid.* **73**, 664 (1994).
[7] S. Kato *et al.*, Phys. Fluids B **5**, 564 (1993).
[8] D. W. Forslund *et al.*, Phys. Rev. A **11**, 679 (1975).
[9] E. S. Weibel, Phys. Fluids **10**, 741 (1967); A. A. Andreev, K. Yu. Platonov, and J.-C. Gauthier, Phys. Rev. E **58**, 2424 (1998).
[10] P. J. Catto *et al.*, Phys. Fluids **20**, 704 (1977); T. Y. Brian Yang *et al.*, Phys. Plasmas **2**, 3146 (1995).
[11] T.-Y. Brian Yang *et al.*, Phys. Plasmas **3**, 2702 (1996).
[12] D. A. Russell *et al.*, Phys. Rev. Lett. **86**, 428 (2001).
[13] M. D. Perry *et al.*, Science **264**, 917 (1994).
[14] E. Tokunaga *et al.*, Opt. Lett. **17**, 1131 (1992); P. Blanc *et al.*, J. Opt. Soc. Am. B **13**, 118 (1996).
[15] R. Lichters *et al.*, Phys. Plasmas **3**, 3425 (1996).
[16] H. M. Milchberg and R. R. Freeman, Phys. Fluids B **2**, 1395 (1990); W. Rozmus *et al.*, Phys. Plasmas **3**, 360 (1996).
[17] S. Hokin, Rev. Sci. Instrum. **63**, 5041 (1992); T. W. Phillips *et al.*, *ibid.* **70**, 1213 (1999); S. P. Hatchett *et al.*, Phys. Plasmas **7**, 2076 (2000). P. Zhang *et al.*, Phys. Rev. E **57**, R3746 (1998); L. M. Chen *et al.*, *ibid.* **63**, 036403 (2001).
[18] D. F. Price *et al.*, Phys. Rev. Lett. **75**, 252 (1995).
[19] W. L. Kruer, *The Physics of Laser Plasma Interaction* (Addison-Wesley, New York, 1988).
[20] E. Lefebvre and G. Bonnaud, Phys. Rev. E **55**, 1011 (1997).
[21] J. Zhang *et al.*, Phys. Rev. Lett. (to be published).
[22] A. Simon *et al.*, Phys. Fluids **26**, 3107 (1983).
[23] J. P. Matte *et al.*, Phys. Rev. Lett. **72**, 1208 (1994).
[24] T. Feurer *et al.*, Phys. Rev. E **56**, 4608 (1997).
[25] H. Ruhl *et al.*, Phys. Rev. Lett. **82**, 2095 (1999).
[26] P. Gibbon, Phys. Rev. Lett. **76**, 50 (1996).